Autofluorescence of epithelial tissue: single-photon versus two-photon excitation

Wei Zheng
Yicong Wu*
Dong Li
Jianan Y. Qu
Hong Kong University of Science and Technology
Department of Electronic and Computer Engineering
Hong Kong

Abstract. We instrumented a combined fluorescence spectroscopy and imaging system to characterize the single- and two-photon excited autofluorescence in epithelial tissue. Single-photon fluorescence (SPF) are compared with two-photon fluorescence (TPF) measured at the same location in epithelial tissue. It was found that the SPF and TPF signals excited at corresponding wavelengths are similar in nonkeratinized epithelium, but the SPF and TPF spectra in the keratinized epithelium and the stromal layer are significant different. Specifically, the comparison of SPF signals with TPF signals in keratinized epithelial and stromal layers shows that TPF spectral peaks always have about 15-nm redshift with respect to SPF signals, and the TPF spectra are broader than SPF spectra. The results were generally consistent with the SPF and TPF measurements of pure nicotinamide adenine dinucleotide, flavin adenine dinucleotide, keratin and collagen, the major fluorophores in epithelium and stroma, respectively. The double peak structure of TPF spectra measured from keratinized layer suggests that there may be an unknown fluorophore responsible for the spectral peak in the long wavelength region. Furthermore, the TPF signals excited in a wide range of wavelengths provide accurate information on epithelial structure, which is an important advantage of TPF over SPF spectroscopy in the application for the diagnosis of tissue pathology.
[DOI: 10.1117/1.2975866]

Keywords: autofluorescence; confocal microscopy; two-photon spectroscopy; epithelial tissue.

Paper 08037R received Jan. 27, 2008; revised manuscript received Apr. 17, 2008; accepted for publication Apr. 17, 2008; published online Sep. 10, 2008.

1 Introduction

Most human cancers arise from the epithelium, a cell-rich superficial tissue, because of frequent exposure to various forms of physical and chemical damages. The development of precancer in epithelium is associated with a variety of physiological and morphologic alterations about the epithelial cells, for example, the increased metabolic activity, the increased cell density and nuclear size, and the loss of cellular maturation.[1,2] The presence of epithelial precancer is also accompanied with architectural changes in the underlying stroma, including neovascularization and slow destruction of the collagen cross-link by protease.[3,4] Therefore, sensing of these physiological and morphologic changes can provide diagnostic information for the detection of precancerous lesions.

Autofluorescence spectroscopy has been a widely explored technique for *in vivo* and noninvasive diagnosis of epithelial precancers over the past two decades.[5,6] It has been reported that the increased tissue metabolic activity associated with the progression of epithelial precancer leads to an increase of nicotinamide adenine dinucleotide (NADH) fluorescence and decrease in ratio of flavin adenine dinucleotide (FAD) over NADH fluorescence that is related to the redox ratio.[7–9] On the other hand, the changes of tissue morphology associated with the process of carcinogenesis, such as thickening of the epithelium and destruction of collagen fibers in the connective tissue, result in the decrease of collagen fluorescence.[7,10] These changes of intrinsic fluorescence properties can be used to differentiate epithelial precancers from normal tissues.

Epithelial tissue has a complicated structure. The fluorescence signal measured with a conventional spectroscopic method is a mixture of signals from different tissue layers. It was demonstrated that keratin fluorescence from topmost keratinized epithelial layer and collagen fluorescence from stroma create serious interferences in extracting the epithelial fluorescence that is weak, but important for the characterization of tissue pathology.[11,12] Furthermore, the fluorescence of keratin and collagen have similar spectral characteristics. It is challenging to distinguish the collagen signal, one of intrinsic biomarker for precancer detection, from the keratin fluorescence.[11,13] Therefore, single-photon fluorescence (SPF) confocal and two-photon fluorescence (TPF) techniques that

*Current address: Department of Bioengineering, University of Washington, Seattle, WA 98195-5061.
Address all correspondence to Jianan Y. Qu, Department of Electronic and Computer Engineering, Hong Kong University of Science and Technology, Clear Water Bay, Kowloon, Hong Kong. Tel: 852-2358-8541; Fax: 852-2358-1485; E-mail: eequ@ust.hk.

1083-3668/2008/13(5)/054010/8/$25.00 © 2008 SPIE

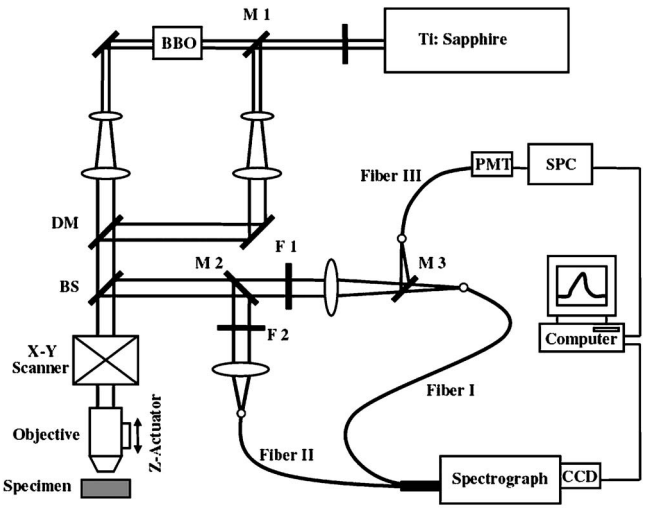

Fig. 1 Combined spectroscopy and imaging system. M1, M2, M3: movable mirrors; F1: long pass filter, F2: short pass filter; DM: dichroic mirror; BS: beam splitter.

provide optical sectioning and depth-resolved spectroscopy are desirable to separate the autofluorescence from different layers and extract more accurate diagnostic information for the assessment of tissue pathology.

Our previous studies showed that depth-resolved autofluorescence measured by using SPF confocal technique provided detailed information on the layered structures and biochemistry of the examined epithelial tissues.[11,13] Furthermore, we found that the depth-resolved SPF spectroscopy could sense the increase of metabolic activity in the epithelial layer of early cervical cancer lesions.[14] In the studies of two-photon spectroscopy of epithelial tissue, it was demonstrated that the information on detailed structure and biochemistry of epithelial tissue also could be extracted from the TPF and second harmonic generation (SHG) signals.[15,16]

The confocal fluorescence techniques based on single-photon excitation have been compared with two-photon techniques in optical sectioning capability, lateral and axial resolution limits, penetration depth, photodamage, and such.[17–20] Also, it was shown that SPF and TPF spectra of pure NADH and FAD, the major fluorophores in epithelial tissue, were almost identical.[21] However, the spectral characteristics of single- and two-photon excited autofluorescence have not been systematically investigated. It is still not clear whether the SPF and TPF signals measured from the same location of tissue are equivalent. In this study, we investigate the spectral characteristics of single- and two-photon excited autofluorescence in epithelial tissue in a wide range of excitation wavelengths. The results could reveal whether the confocal and TPF spectroscopy produce equivalent information on the biochemistry and biomorphology of tissue. Furthermore, the results provide important basis to choose the optimal excitation wavelengths and emission wavelength bands for SPF and TPF imaging of epithelial tissue.

2 Methods and Materials

The schematic diagram of the combined fluorescence spectroscopy and imaging system is shown in Fig. 1. Briefly, a tunable femtosecond Ti:Sapphire laser (Mira900-S, Coherent, Santa Clara, California) and its SHG were used to excite two-photon signals (TPF/SHG) and SPF signals, respectively. The selection of excitation for two-photon or single-photon measurements was done by simply removing or restoring the removable mirror M1. Two excitation beams virtually combined by a dichroic mirror were focused into the tissue sample with a water immersion objective lens (40×, 1.15 numeric aperture, Olympus, Center Valley, Pennsylvania). The single-photon and two-photon signals were excited at the same location in the tissue sample, respectively. The excitation beams were scanned in a 100×100-μm sampling area by a pair of galvo-mirror scanners. A bifurcated fiber bundle with two single fibers (Fiber I and Fiber II) was used to conduct the backscattered SPF and TPF/SHG signals to a spectrograph for spectral analysis, respectively. A cooled charge-coupled Device (NTE/CCD-1340/400-EMB, Roper Scientific, Trenton, New Jersey) was used to record the fluorescence and SHG signals. The other fiber (Fiber III) conducted the SPF signal to a single-photon counting photomultiplier tube to form the confocal fluorescence image of sampled tissue area at certain depth. Fibers I and III with small cores were used as pinholes to collect confocal SPF signals, but Fiber II with a large core was used to effectively collect TPF/SHG signals. The mirror M2 reflected TPF/SHG signals to Fiber II for two-photon measurements and it was removed in the SPF measurements. The mirror M3 reflected the SPF signals to take confocal fluorescence images, and it was removed when measuring the confocal SPF spectral signal. A shortpass filter (ET700sp Chroma, Technology, Rockingham, Vermont) was used to reject the near-infrared excitation of wavelength over 700 nm in all the TPF measurements. In the SPF measurement, we always chose a longpass filter of cut-off wavelength about 30 nm longer than the excitation wavelength to reject the excitation laser. The axial and lateral resolutions were about 3.5 and 0.75 μm for SPF and 3 and 0.5 μm for TPF, respectively. The wavelength and intensity response of the spectrometry system were calibrated by using a mercury lamp (HG-1, Ocean Optics, Dunedin, Florida) and tungsten halogen light source (LS-1, Ocean Optics), respectively.

To avoid photobleaching, the excitation power was controlled in the ranges from 10 to 40 μW for SPF measurements and from 20 to 40 mW for TPF measurements, respectively. We measured the spectra at very low excitation power levels (a few microwatts for SPF and a few milliwatts for TPF, respectively) and found no obvious difference in spectral characteristics except poorer signal-to-noise ratio. When measuring the depth-resolved SPF or TPE spectra from a sample, the signal was averaged over the sampling area at the certain depth to shorten the exposure time and achieve high signal-to-noise ratio. The exposure time for each measurement of SPF or TPF/SHG spectral signal was 3 s. The exposure time to take a 100×100-μm fluorescence confocal image was about 30 s.

The tissue samples used in this study were esophageal tissues freshly excised from 12 experimental rabbits. All samples were rinsed briefly with phosphate buffered saline solution to remove the residual blood before the measurements. A coverslip was placed on top of the tissue sample to

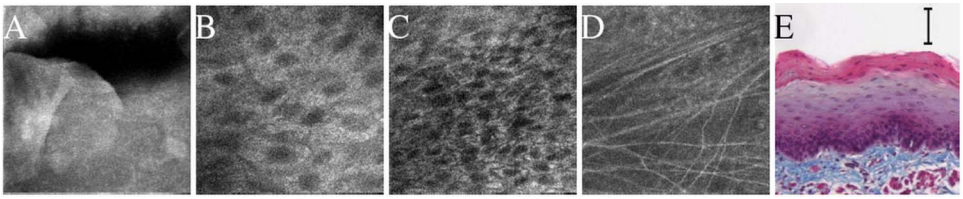

Fig. 2 Confocal autofluorescence images of esophageal tissue at different depths. (a) 5 μm; (b) 65 μm; (c) 85 μm; (d) 105 μm; (e) corresponding Masson-stained histology (vertical scale bar: 50 μm). Excitation wavelength: 405 nm.

keep the surface flat. A drop of phosphate buffered saline solution was applied between the tissue surface and coverslip to prevent dehydration of sample. The measurements were taken from four different places within each sample. All the measurements were completed within 4 h after the tissue samples were excised from the animals. The samples were fixed with formalin after fluorescence measurements. Slides made from the fixed samples were stained with hematoxylin and eosin and Masson stains for histological evaluation. To understand the characteristics of the SPF and TPF signals from the epithelial tissue, we also measured the SPF and TPF spectral signals of pure NADH, FAD, keratin and collagen solution, which are the major fluorophores in epithelium and stromal layer, respectively. These chemical solutions or powder were purchased from Sigma-Aldrich (St. Louis, Missouri).

The previous study showed that esophageal epithelium is generally keratinized.[13] The epithelial tissue consists of three layers: keratinized epithelium, nonkeratinized epithelium, and stroma. To investigate the characteristics of single- and two-photon excited signals, it is important to accurately determine which layer the signals are measured from. In this study, we used three different methods to identify the structure of examined epithelial tissue. The depth-resolved confocal autofluorescence images obtained by the system shown in Fig. 2 were used to identify three tissue layers based on their difference in morphology. In addition, the confocal SPF excited at 355 nm and two-photon excited SHG were used to cross-check the results of confocal fluorescence imaging in separation of keratinized from nonkeratinized epithelial layer and the separation of epithelium from underlying stroma, respectively.[11,15] Finally, the structure of the examined tissue sample was further confirmed by using hematoxylin and eosin and Masson stained histology.

3 Results and Discussions

Typical confocal autofluorescence images of an esophageal sample are shown in Figs. 2(a)–2(d). The image of topmost layer [Fig. 2(a)] shows flocculent structures without nuclei, indicating the keratinization of epithelium. Underlying the keratinized layer, the epithelial cells with dark nuclei surrounded by cytoplasm of strong fluorescence were observed. The images of nonkeratinized epithelium are shown in Figs. 2(b) and 2(c). As can be seen, the nuclear density increases with the increase of sampling depth until the stroma was reached. Finally, the stromal layer was identified with the fibrillar collagens below the basal cells as shown in Fig. 2(d). The tissue structure identified by using the results of confocal fluorescence imaging was completely consistent with the corresponding histology shown in Fig. 2(e), in which the topmost keratinized epithelial layer, the nonkeratinized layer formed with mature epithelial cells, and the stromal layer with blue-stained collagen fibers are clearly identified, respectively.

The SPF signals excited at the representative wavelengths—355, 375, 395, and 415 nm—and TPF/SHG signals excited at four corresponding near-infrared wavelengths are shown in Fig. 3. The structures of examined epithelial tissues were determined as the topmost keratinized epithelial layer, the nonkeratinized epithelial layer in the middle, and the underlying stromal layer based on the method described in Sec. 2. Each pair of SPF and TPF spectra at the corresponding single- and two-photon excitation wavelengths were the average over the measurements from the samples obtained from 12 experimental rabbits. As shown in Figs. 3(c) and 3(d), the SPF spectra of nonkeratinized epithelial tissue excited at 355 and 415 nm and the TPF spectra excited at the corresponding wavelengths at 710 and 830 nm are almost identical because the fluorescence excited at the wavelengths may be dominated by NADH and FAD signals, respectively.[10,13] However, the SPF and TPF spectra excited at the wavelengths in between are different because the signals are the mixture of NADH and FAD fluorescence and the efficiencies of single-photon excitation for NADH and FAD fluorescence are different from those of two-photon excitation.[21] It should be noted that the fluorescence spectral characteristics of three layers were not found to be depth-dependent except in the transition zone between two adjacent layers. The fluorescence in the transition zone of thickness less than 20 μm is a mixture of the signals from two adjacent layers. Therefore, in the calculation of averaged fluorescence spectra of three layers, the signals measured from the transition zones are not included.

Remarkable differences in the spectral characteristics between SPF and TPF spectra were observed in the topmost keratinized epithelium and the underlying stromal layers. As can be seen in Figs. 3(a) and 3(b), the TPF spectra of keratinized epithelium are significantly broader than SPF spectra excited at corresponding wavelengths. In addition to a redshift of TPF signals from SPF signals, a two-peak structure appears in the TPF spectra. For example, the TPF spectrum excited at 750 nm has two peaks located around 450 and 530 nm, respectively. In the stromal layer, an almost constant redshift and spectral broadening of TPF signals compared with SPF signals excited at corresponding wavelengths were observed as shown in Figs. 3(e) and 3(f). The redshift and spectral broadening are about 15 and 10 nm, respectively. The strong SHG measured in stromal layer was contributed from collagen fibers.[15,16]

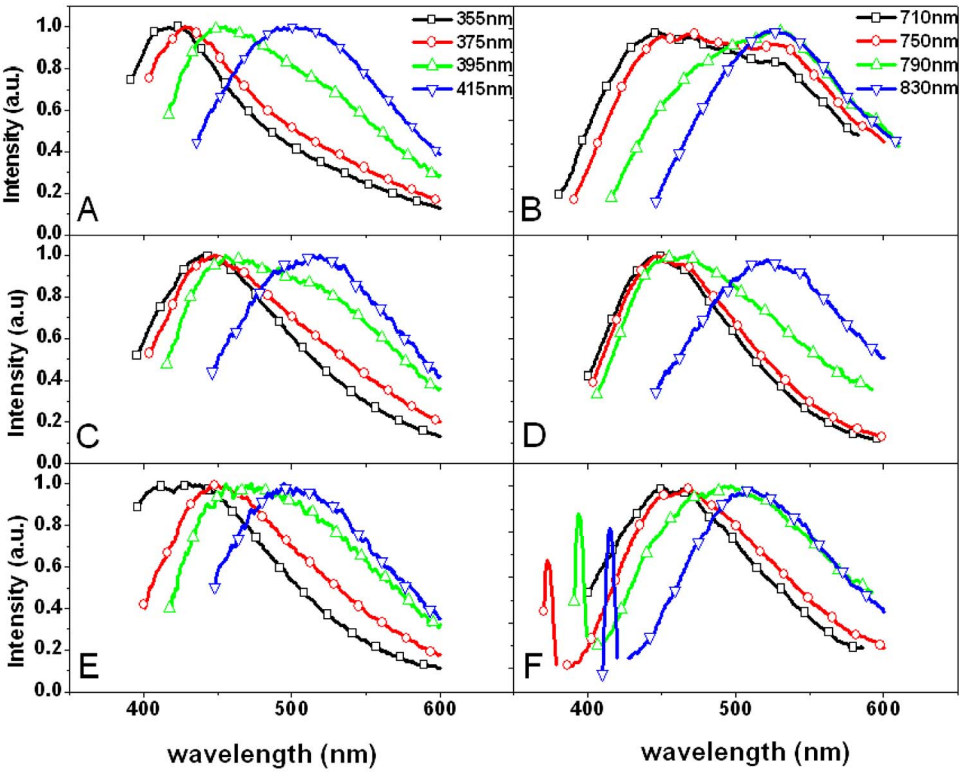

Fig. 3 Normalized single-photon excited spectral signals (left side) and two-photon excited spectral signals (right side) from different tissue layers. (a, b) Keratinized epithelium; (c, d): nonkeratinized epithelium; (e, f) stromal layer. The amplitudes of SHG in (f) are reduced by a factor of 20.

To better understand the spectral characteristics of SPF and TPF signals, we measured the fluorescence of pure chemicals of NADH, FAD, keratin and collagen solutions, which are the major fluorophores in the epithelium and stromal layers, respectively.[12,13] The results are shown in Fig. 4. As can be seen, the SPF and TPF spectra of NADH or FAD are identical, except the SPF and TPF spectra of NADH excited at 415 and 830 nm, respectively. It is known that the absorption and excitation efficiency of NADH drops rapidly with increase of excitation wavelength.[21,22] The SPF and TPF signals of NADH excited at 415 and 830 nm are at least a factor of 10 weaker than those excited at shorter wavelengths and the spectral lineshapes are different, suggesting that they may have originated from an impurity in the NADH solution. Overall, the fluorescence emission spectra of NADH and FAD are independent of both the excitation wavelength and the excitation model of single- or two-photon, which are consistent with the results of previous studies.[21,22] The results confirm that the SPF spectra of nonkeratinized epithelium excited at 355 and 415 nm are almost identical to the TPF spectra excited at 710 and 830 nm, respectively, because NADH and FAD are dominant fluorophores in nonkeratinized epithelium.

The fluorescence spectral characteristics of collagen and keratin exhibit significant difference from NADH and FAD. As shown in Figs. 4(c)–4(f), the fluorescence peaks of keratin and collagen redshift constantly with increasing of excitation wavelengths for both single- and two-photon excitation. The TPF spectra are all redshifted and the bandwidths are all broadened compared with the SPF spectra at the corresponding excitation wavelengths. For example, the peak location and full width at half maximum of the SPF spectrum of collagen excited at 395 nm are at 460 and about 110 nm, respectively. The peak location and bandwidth of TPF signal excited at 790 nm changes to 475 and 140 nm, respectively. The peak location and full width at half maximum of the SPF spectrum of keratin excited at 395 nm are at 470 and about 125 nm, respectively. The peak location and bandwidth of TPF signal excited at 790 nm are 490 and 145 nm, respectively. Strong SHG signal was measured from collagen, but no SHG was observed from the keratin sample. The noisier TPF spectra of keratin and collagen compared with SPF spectra may be due to the lower TPF excitation efficiency.[23,24]

Although Xu and Webb[25] reported no difference in the emission spectra between SPF and TPF spectra for the five fluorescent dyes they investigated, there were cases in which differences were observed.[26,27] Bestvater et al.[26] revealed that TPF spectra of more than 20 dyes exhibited a redshift compared with the SPF spectra. Our results showed that the SPF and TPF spectra of coenzyme fluorophores (NADH, FAD) are identical. However, the TPF spectra of keratin and collagen, the structure proteins with much higher molecular weight than NADH and FAD, exhibit significant redshift and spectral broadening in comparison with the SPF spectra. The mechanisms causing the differences are not clear and undergoing investigation.

Comparing the single- and two-photon signals of stromal layer shown in Figs. 3(e) and 3(f) with the signals of pure collagen shown in Figs. 4(e) and 4(f), respectively, the spectral characteristics of fluorescence (SPF and TPF) and SHG signals from the stromal layer can be well explained by col-

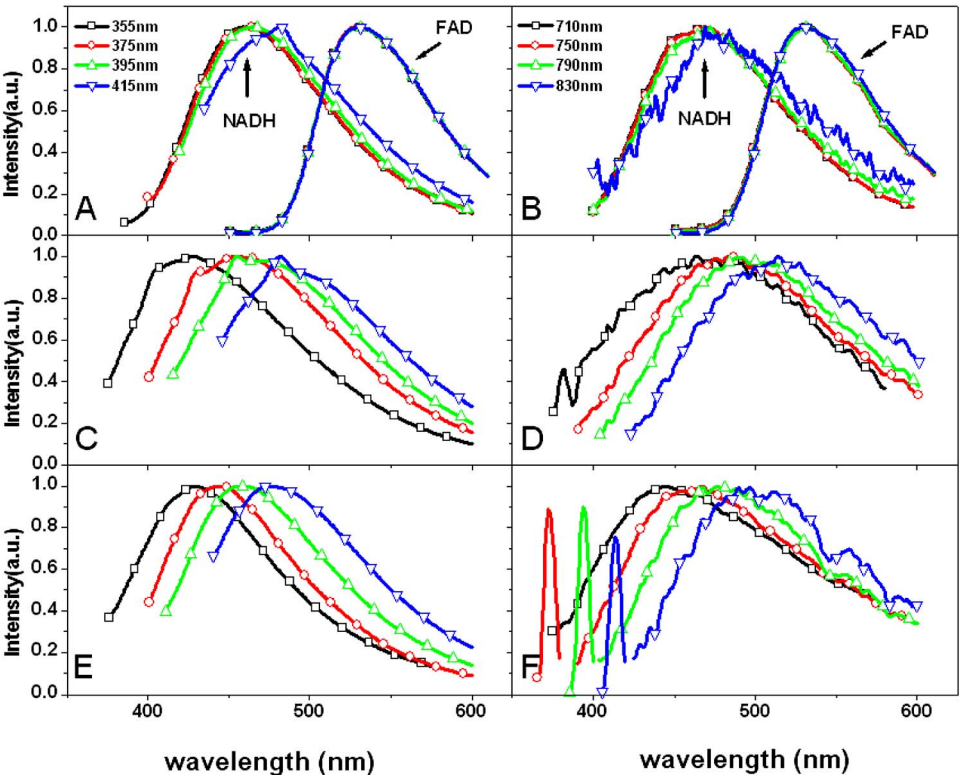

Fig. 4 Normalized single-photon excited spectral signals (left side) and two-photon excited spectral signals (right side) of different fluorophores. (a, b) NADH (peak at 460 nm) and FAD (peak at 530 nm); (c, d) keratin; (e, f) collagen. The small peaks in (a) and (c) are Raman spectra of water. The amplitudes of SHG in (f) are reduced by a factor of 10.

lagen signals. Though slight redshift of stromal spectra from the pure collagen spectra was observed, the shift of fluorescence peak may be from two possible sources. First, the solvent effect may cause the spectral shift because collagen signals were measured from water solutions instead of the chemical environment similar to connective tissue. Second, coexistence of other fluorophores in stroma may contribute to the shift. For example, although the collagen is believed to be the major fluorophore in the stroma, NADH and elastin were also observed in the fibroblast and connective tissue.[8,16]

The signals of keratinized epithelium were found to be different from those of pure keratin. Though the redshift of TPF from SPF spectra in the keratinized layer can be explained by the pure keratin signals, the TPF spectra of keratinized epithelium are broader than those of pure keratin and a two-peak structure appears in the TPF spectra of keratinized epithelium. One possible explanation for the difference is that the keratin profile in examined esophageal epithelial tissue may be different from that of pure keratin solution that was extracted from human skin. There are 21 different types of keratin/cytokeratin. The profile of keratin in epithelium varies from organ to organ.[28,29] Furthermore, it is known that the topmost epithelial layer is formed from the division, differentiation, and slough of the basal cells. As the cells migrate to the surface, not only the keratin is produced, but also another small organelle such as lamellar granule is accumulated.[16] In particular, various lipids are packaged in lamellar granules. It was reported that several types of the lipids, such as lipofuscin and phosphoslipid, emitted an intense yellow autofluorescence that peaked about 540 nm.[30–32] Thus, it is possible that the fluorescence of lipids may contribute to the two-peak structure in the fluorescence spectra of the keratinized epithelial layer.[16,32] It was noted that the two-peak structure is not obvious in SPF spectra. This may be due to the difference in fluorescence excitation efficiency for the fluorophore with a peak at the longer wavelength between single- and two-photon excitation models.

Because the SPF and TPF spectral characteristics vary from layer to layer in epithelial tissue, a simple ratio technique could be used to identify the tissue structure. Specifically, the tissue layers could be separated from each other based on the ratio of the SPF or TPF signal in a short wavelength band over the signal in a long wavelength band. The optimal short- and long-wavelength bands could be identified by using the differential spectra between the normalized mean spectra of three layers.[33,34] We calculated the differential spectrum between keratinized epithelial layer (K) and nonkeratinized epithelial layer (E), $I_{K\text{-}E}$, and the differential spectrum between nonkeratinized epithelial layer and stromal layers (S), $I_{E\text{-}S}$, respectively. The optimal short and long wavelengths to separate the K layer from the E layer were determined by the locations of two extrema in the $I_{K\text{-}E}$ spectrum in the short- and long-wavelength regions, respectively. Similarly, the optimal wavelengths to separate the E layer from the S layer were determined by the locations of two extrema in the $I_{E\text{-}S}$ spectrum, respectively. As an example, representative $I_{K\text{-}E}$ and $I_{E\text{-}S}$ spectra for SPF and TPF excited at correspond-

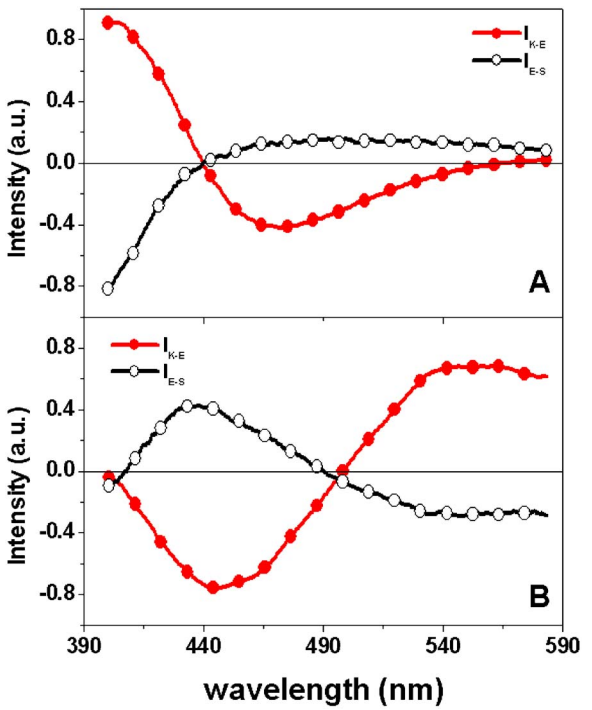

Fig. 5 Representative SPF and TPF differential spectra between keratinized epithelial layer (*K*) and nonkeratinized epithelial layer (*E*), $I_{K\text{-}E}$, and between nonkeratinized epithelial layer and stromal layer (*S*), $I_{E\text{-}S}$. The excitation wavelengths for SPF and TPF are 355 and 710 nm, respectively.

ing wavelengths are shown in Fig. 5. The maxima and minima in the differential spectra can be clearly identified.

By setting the wavelength band to 20 nm, the ratio values of optimal short over long wavelength bands for all SPF and TPF spectral signals measured from different tissue layers were calculated. The separation between adjacent layers based on the difference in their ratio values were evaluated by using Student's *t* test. Thus, two *p* values were obtained for the separation of the *K* layer from the *E* layer and the *E* layer from the *S* layer, respectively. The accuracy of global separation between three layers was then determined by the separation of two adjacent layers that produced greater *p* values. It was found that the optimal pairs of short- and long-wavelength bands to separate the *K* layer from the *E* layer and that to separate the *E* layer from the *S* layer were slightly different. In practice, a ratio technique should only use one pair of wavelength bands. We chose the pair of wavelength bands that produced the smallest *p* value for the separation of two adjacent layers. This means that this pair of wavelengths was not the optimal pair of wavelength bands to separate the other two adjacent layers. However, it was found that the *p* value for separation of other two adjacent layers with the nonoptimal wavelength bands was still smaller, suggesting that the accuracy in global separation among the three layers was not sacrificed.

The optimal pairs of wavelength bands at representative excitation wavelengths are listed in Table 1. Ratio values in each layer and *p* values in separation of adjacent layers are also listed in the same table. As shown in the table, the three-layer structure can be well identified using SPF when excitation is at a short wavelength. However, the *E* layer cannot be separated from the underlying *S* layer when excitation was tuned to be longer than 375 nm and the same tissue layer cannot be separated from topmost *K* layer when excitation wavelength is longer than 395 nm. However, the three-layer structure of epithelial tissue can be separated by the ratios calculated from TPF spectral signals with the excitation in the range from 710 to 810 nm. Though the separation of the *E* layer from the *S* layer is marginally good at 710-nm excitations because the *p* value is close to 0.01, the *S* layer can be accurately identified by SHG signals. This is a significant advantage of two-photon excitation.

Our previous studies[13,35] revealed that with the excitation at 405 nm, the single-photon excited NADH and FAD fluo-

Table 1 Optimal wavelength bands for determination of three-layer structure.

			Ratio Value			*p* Value	
	λ_{ex} (nm)	$\lambda_{short}/\lambda_{long}$ (nm)	K	E	S	*K* vs. *E*	*E* vs. *S*
SPF	355	405/470	1.57±0.12	0.79±0.21	1.21±0.19	2.09×10^{-12}	1.12×10^{-5}
	375	410/480	1.32±0.18	0.69±0.09	0.75±0.08	2.99×10^{-10}	9.08×10^{-2}
	395	430/480	0.90±0.14	0.80±0.15	0.73±0.09	9.21×10^{-2}	2.11×10^{-1}
	405	450/540	1.00±0.08	0.96±0.14	1.20±0.22	5.80×10^{-1}	3.23×10^{-2}
TPF	710	435/540	1.37±0.23	2.50±0.60	1.87±0.24	4.01×10^{-6}	7.56×10^{-3}
	750	430/540	1.06±0.21	2.20±0.42	1.43±0.26	1.12×10^{-7}	9.52×10^{-5}
	790	435/540	0.53±0.09	1.50±0.43	0.81±0.19	3.02×10^{-9}	8.42×10^{-6}
	810	450/540	0.56±0.10	1.21±0.18	0.84±0.17	4.09×10^{-6}	2.75×10^{-3}

λ_{ex}: excitation wavelength; λ_{short}, λ_{long}: central wavelengths of optimal short- and long-wavelength bands, respectively; *K*: keratinized epithelium; *E*: nonkeratinized epithelium; *S*: stromal layer; bandwidth is 20 nm.

rescence of epithelial cells reached a balanced level, and the ratio of fluorescence bands at 450 nm over 530 nm could produce a good estimation of epithelial metabolism. However, SPF excited at 405 nm cannot resolve the structure of epithelial tissue. By contrast, the TPF signal excited at 810 nm, which is equivalent to SPF excited at 405 nm, can resolve the three-layer structure of epithelial tissue and potentially sense the metabolic activity in the nonkeratinized epithelial layer at the same time. In addition, the SHG signal excited at 810 nm in the stromal layer can improve the accuracy to separate the epithelial layer from the stroma and reveal the collagen content, which is an important biomarker of precancer development. Therefore, our results demonstrate that a two-photon spectroscopic technique will ultimately produce more accurate information for the diagnosis of tissue pathology.

4 Conclusion

We conducted a systematic investigation of SPF and TPF/SHG signals in epithelial tissue. The results showed that SPF and TPF from nonkeratinized epithelial tissue may produce equivalent information because SPF and TPF signals of NADH and FAD, the major fluorophores in nonkeratinized epithelium, are identical. However, the spectral characteristics of SPF and TPF in keratinized epithelial layer and stromal layers are significantly different, which are consistent with the study of single- and two-photon excited signals from pure keratin and collagen. The stromal signals could be well understood as collagen is the dominant fluorophore in the layer, but it is more complicated to explain the SPF and TPF signals in keratinized epithelium because keratin may not be the only fluorophore in keratinized epithelium, and the keratin profile in the examined esophageal epithelium may be different from that of keratin solution used in this study. Finally, our study demonstrated that two-photon excited signals can clearly identify the three-layer structure of epithelial tissue. A two-photon spectroscopic technique can potentially sense three important parameters associated with early cancer development: the thickness of epithelial layer, metabolic activity in nonkeratinized epithelium, and destruction of the collagen network in the stroma by protease. It should be noted that the spectroscopic technique does not provide as much information on tissue morphology as the microscopic imaging approach. However, the spectroscopic technique takes much less time to acquire high quality spectral signals. This makes it practical in the application for clinical diagnosis in which rapid measurement is a critical requirement.

Acknowledgments

The authors gratefully acknowledge the support from (1) Hong Kong Research Grants Council through grant HKUST6408/05M and (2) HKUST Research Project Competition through the grant RPC06/07.EG06.

References

1. C. W. Boone, J. W. Bacus, J. V. Bacus, V. E. Steele, and G. J. Kelloff, "Properties of intraepithelial neoplasia relevant to cancer chemoprevention and the development of surrogate end points for clinical trials," *Proc. Soc. Exp. Biol. Med.* **216**, 151–165 (1997).
2. G. I. Evan and K. H. Vousden, "Proliferation, cell cycle and apoptosis in cancer," *Nature (London)* **411**, 342–348 (2001).
3. A. Dellas, H. Moch, E. Schultheiss, G. Feichter, A. C. Almendral, F. Gudat, and J. Torhorst, "Angiogenesis in cervical neoplasia: microvessel quantitation in precancerous lesions and invasive carcinomas with clinicopathological correlations," *Gynecol. Oncol.* **67**, 27–33 (1997).
4. Y. A. Declerck, "Interactions between tumour cells and stromal cells and proteolytic modification of the extracellular matrix by metalloproteinases in caner," *Eur. J. Cancer* **36**, 1258–1268 (2000).
5. N. Ramanujam, "Fluorescence spectroscopy of neoplastic and non-neoplastic tissues," *Neoplasia* **2**, 89–117 (2000).
6. D. C. G. DeVeld, M. J. H. Witjes, H. J. C. M. Sterenborg, and J. L. N. Roodenburg, "The status of in vivo autofluorescence spectroscopy and imaging for oral oncology," *Oral Oncol.* **41**, 117–131 (2005).
7. I. Georgakoudi, B. C. Jacobson, M. G. Muller, E. E. Sheets, K. Badizadegan, D. L. Carr-Locke, C. P. Crum, C. W. Boone, R. R. Dasari, J. V. Dam, and M. S. Feld, "NAD(P)H and collagen as *in vivo* quantitative fluorescent biomarkers of epithelial precancerous changes," *Cancer Res.* **62**, 682–687 (2002).
8. K. Sokolov, J. Galvan, A. Myakov, A. Lacy, R. Lotan, and R. Richards-Kortum, "Realistic three-dimensional epithelial tissue phantoms for biomedical optics," *J. Biomed. Opt.* **7**, 148–156 (2002).
9. B. Chance, B. Schoener, R. Oshino, F. Itshak, and Y. Nakase, "Oxidation-reduction ratio studies of mitochondria in freeze-trapped samples-NADH and flavoprotein fluorescence signals," *J. Biol. Chem.* **254**, 4764–4771 (1979).
10. R. Drezek, K. Sokolov, U. Utzinger, I. Boiko, A. Malpica, M. Follen, and R. Richards-Kortum, "Understanding the contribution of NADH and collagen to cervical tissue fluorescence spectra: modeling, measurements and implications," *J. Biomed. Opt.* **6**, 385–396 (2001).
11. Y. Wu, P. Xi, and J. Y. Qu, "Depth-resolved fluorescence spectroscopy reveals layered structure of tissue," *Opt. Express* **12**, 3218–3223 (2004).
12. S. K. Chang, N. Marin, M. Follen, and R. Richards-Kortum, "Model-based analysis of clinical fluorescence spectroscopy for in vivo detection of cervical intraepithelial dysplasia," *J. Biomed. Opt.* **11**, 024008 (2006).
13. Y. Wu and J. Y. Qu, "Autofluorescence spectroscopy of epithelial tissue," *J. Biomed. Opt.* **11**, 054023 (2006).
14. Y. Wu, P. Xi, and J. Y. Qu, "Depth-resolved fluorescence spectroscopy of normal and dysplastic cervical tissue," *Opt. Express* **13**, 382–388 (2005).
15. Y. Wu and J. Y. Qu, "Two-photon autofluorescence spectroscopy and second-harmonic generation of epithelial tissue," *Opt. Lett.* **30**, 3045–3047 (2005).
16. J. A. Palero, H. S. deBruijn, A. V. van den Heuvel, H. J. C. M. Sterenborg, and H. C. Gerritsen, "Spectrally resolved multiphoton imaging of in vivo and excised mouse skin tissues," *Biophys. J.* **93**, 992–1007 (2007).
17. V. E. Centonze and J. G. White, "Multiphoton excitation provides optical sections from deeper within scattering specimens than confocal imaging," *Biophys. J.* **75**, 2015–2024 (1998).
18. B. R. Masters and P. T. C. So, "Multi-photon excitation microscopy and confocal microscopy imaging of in vivo human skin: a comparison," *Microsc. Microanal.* **5**, 282–289 (1999).
19. M. Gu and C. J. R. Sheppard, "Comparison of 3-dimensional imaging properties between 2-photon and single-photon fluorescence microscopy," *J. Microsc.* **177**, 128–137 (1995).
20. K. Konig, P. T. C. So, W. W. Mantulin, and E. Gratton, "Cellular response to near-infrared femtosecond laser pulses in two-photon microscopes," *Opt. Lett.* **22**, 135–136 (1997).
21. S. Huang, A. A. Heikal, and W. W. Webb, "Two-photon fluorescence spectroscopy and microscopy of NAD(P)H and flavoprotein," *Biophys. J.* **82**, 2811–2825 (2002).
22. W. R. Zipfel, R. M. Williams, R. Christie, A. Y. Nikitin, B. T. Hyman, and W. W. Webb, "Live tissue intrinsic emission microscopy using multiphoton-excited native fluorescence and second harmonic generation," *Proc. Natl. Acad. Sci. U.S.A.* **100**, 7075–7080 (2003).
23. A. Zoumi, A. Yeh, and B. J. Tromberg, "Imaging cells and extracellular matrix in vivo by using second-harmonic generation and two-photon excited fluorescence," *Proc. Natl. Acad. Sci. U.S.A.* **99**, 11014–11019 (2002).
24. A. M. Pena, M. Strupler, T. Boulesteix, and M. C. Schanne-Klein, "Spectroscopic analysis of keratin endogenous signal for skin multiphoton microscopy," *Opt. Express* **13**, 6268–6274 (2005).
25. C. Xu and W. W. Webb, "Measurement of two-photon excitation cross sections of molecular fluorophores with data from

690 to 1050 nm," *J. Opt. Soc. Am. B* **13**, 481–491 (1996).
26. F. Bestvater, E. Spiess, G. Stobrawa, M. Hacker, T. Feurer, T. Porwol, U. Berchner-pfannschmidt, C. Wotzlaw, and H. Acker, "Two-photon fluorescence absorption and emission spectra of dyes relevant for cell imaging," *J. Microsc.* **208**, 108–115 (2002).
27. L. Parma and N. Omenetto, "Fluorescence behavior of 7-hydroxycoumarine excited by one-photon and two-photon absorption by means of a tunable dye laser," *Chem. Phys. Lett.* **54**, 544–546 (1978).
28. R. Moll, W. W. Franke, D. L. Schiller, B. Geiger, and R. Krepler, "The catalog of human cytokeratins: patterns of expression in normal epithelia, tumors and cultured cells," *Cell* **31**, 11–24 (1982).
29. P. G. Chu and L. M. Weiss, "Keratin expression in human tissues and neoplasms," *Histopathology* **40**, 403–439 (2002).
30. N. Ramanujam, "Fluorescence spectroscopy in vivo," in *Encyclopedia of Analytical Chemistry*, R. A. Meyers, Ed., pp. 20–56, J. Wiley & Sons, Chichester (2000).
31. G. E. Eldred, G. V. Miller, W. S. Stark, and L. Feeney-Burns, "Lipofuscin: resolution of discrepant fluorescence data," *Science* **216**, 757–759 (1982).
32. R. Richards-Kortum and E. Sevick-Muraca, "Quantitative optical spectroscopy for tissue diagnosis," *Annu. Rev. Phys. Chem.* **47**, 555–606 (1996).
33. T. VoDinh, M. Panjehpour, B. F. Overholt, and P. Buckley, "Laser-induced differential fluorescence for cancer diagnosis without biopsy," *Appl. Spectrosc.* **51**, 58–63 (1997).
34. N. Vengadesan, P. Aruna, and S. Ganesan, "Characterization of native fluorescence from DMBA-treated hamster cheek pouch buccal mucosa for measuring tissue transformation," *Br. J. Cancer* **77**, 391–395 (1998).
35. Y. Wu and J. Y. Qu, "Combined depth- and time-resolved autofluorescence spectroscopy of epithelial tissue," *Opt. Lett.* **31**, 1833–1835 (2006).